New Polyimides for Gas Separation. 2. Polyimides Derived from Substituted Catechol Bis(etherphthalic anhydride)s

Majdi Al-Masri,[†] Detlev Fritsch,[‡] and Hans R. Kricheldorf*,[†]

Institut für Technische und Makromolekulare Chemie, Bundesstrasse 45, D-20146 Hamburg, Germany; and GKSS Forschungszentrum GmbH, Max-Planck-Strasse, D-21502 Geesthacht, Germany

Received December 10, 1999

ABSTRACT: A new synthetic procedure was elaborated allowing for the preparation of aromatic dianhydrides. Methyl- and/or *tert*-butylcatechols were silylated at the OH groups and the resulting bistrimethylsilyl derivatives were used as nucleophilic reaction partners for 4-chloro- or 4-nitro-*N*-phenylphthalimides. The bis(*o*-etherphthalimides) were transformed into the corresponding bis(*o*-etherphthalic anhydrides) (six known ones, two new ones). For comparison, a trimethyl substituted bis(*p*-etherphthalic anhydride) was prepared using the same route. These dianhydrides were polycondensed with aromatic diamines such as 1,3-diamino-2,4,6-tetramethylbenzene, 1,4-diamino-2,3,5,6-tetramethylbenzene, 3,3′-dimethoxybenzidine, 3,3′,5,5′-tetramethylbenzidine, or 2,2-bis(4-aminophenyl)hexafluoropropane. In total, 21 polyimides were isolated and characterized. The permeabilities and apparent diffusion coefficients of the pure gases He, H_2, N_2, O_2, CO_2, and CH_4 were measured for 12 selected polyimides in a time-lag apparatus at feed pressures below 1 bar. A correlation between the dianhydride monomer structure and gas permeability was found and discussed.

Introduction

Over the past 20 years, polyimides and particularly poly(ether imide)s have found increasing interest as membrane materials for gas separation purposes.[1−5] For almost all technical applications, a high permeability at a "sufficient" selectivity is needed. It is obvious and also proven in several studies that the permeability of a polymeric membrane is directly correlated to its free volume.[6−8] Systematic variations of the chemical structure and calculations have shown that a high free volume and consequently the permeability are favored by the following structural properties: bulky substituents, hindered rotation of aromatic rings (improved backbone stiffness), kinks, and bends. In other words, all structural elements that hinder a dense chain packing favor the permeability.[9] Among the building blocks designed for poly(ether imide)s the bis(etherphthalic anhydride)s **1**, derived from substituted catechols, seem to be particularly attractive, because they combine several useful properties, such as bulky substituents (R = *tert*-butyl), hindered rotation and a kinked nano structure. Such bis(ether anhydride)s have been prepared by Eastmond and co-workers[10] from 4-nitrophthalodinitrile and catecholes via nucleophilic nitrodisplacement reaction. The nitrile groups were then hydrolyzed and the resulting bis(etherpthalic acid)s were cyclized by means of acetic anhydride. A shortcoming of this synthetic pathway is the high cost of 4-nitrophthalodinitrile. Therefore, it was one purpose of the present work to find an alternative strategy for the synthesis of bis(ether anhydride)s, **1**, and second to study the gas separation properties of the polyimides derived from **1** and various aromatic diamines.

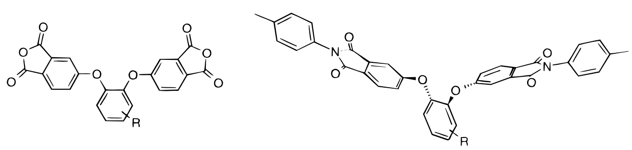

R = CH_3 or $C(CH_3)_3$

1

Experimental Section

4-Chlorophthalic acid (mono Na salt), 4-nitrophthalic acid, 3-methylcatechol, 4-methylcatechol, 4-*tert*-butylcatechol, catechol, 1,3-diamino-2,4,6-trimethylbenzene (MDA), and 3,3′-dimethoxybenzidine (DMOB) were obtained from Sigma-Aldrich (Deisenhofen, Germany) and used as received. 2,2-Bis(4-aminophenyl)hexafluoropropane (6FIPDA) was purchased from Chriskev Co. (Leawood, KS) and sublimed prior to use. 1,4-Diaminotetramethylbenzene and 3,3′,5,5′-tetramethylbenzidine were purchased from Fluka Chem. (Buchs, Switzerland) and sublimed prior to use. Morpholine, chlorotrimethylsilane and potassium carbonate were gifts of Bayer AG (Leverkusen, Germany) and used as received. *N*-Methylpyrrolidone (NMP) was a gift of BASF AG (Ludwigshafen, Germany) and was distilled over P_4O_{10} prior to use.

4-Chlorophthalic Anhydride. Monosodium 4-chlorophthalate (0.2 mol) was stirred at 50 °C with 2 M aqueous HCl (400 mL). Two hours after complete dissolution, the aqueous phase was extracted 4 times with 100 mL portions of ethyl acetate. The combined organic extracts were dried with Na_2SO_4 and evaporated. The residue was then refluxed for 1 h with acetic anhydride (150 mL), and finally the product was isolated by distillation in vacuo. Yield: 84%. Mp: 67−68 °C (lit. mp: 67−68 °C[11]).

The 4-nitrophthalic acid was dehydrated analogously. Yield: 91%. Mp: 119−121 °C (lit. mp: 120−121.5 °C[12]).

4-Chloro-*N*-phenylphthalimide (3a). 4-Chlorphthalic anhydride (0.1 mol) was dissolved in glacial acetic acid (250 mL), and aniline (0.105 mol) was added. The suspension formed after a few minutes yielded a clear solution after 3 h of reflux. The product, which precipitated after cooling with ice, was isolated by filtration, dried in vacuo, and recrystallized from toluene. Yield: 89%. Mp: 189−191 °C (lit. mp: 189.5−191 °C[13]).

[†] Institut für Technische und Makromolekulare Chemie.
[‡] GKSS Forschungszentrum GmbH.

10.1021/ma9920745 CCC: $19.00
Published on Web 08/26/2000

Table 1. Yields and Properties of the Silylated Diols

diol	yield (%)	$n_D 20^\circ$ or mp (°C)	mol formula (mol wt)	elemental analyses	C	H	^{1}H NMR ($CDCl_3$/TMS), δ (ppm)
2a	87	1.4745	$C_{13}H_{24}O_2Si_2$	calcd	58.18	9.02	0.23 (s, 9H), 0.27 (s, 9H), 2.19 (s, 3H), 6.65−6.82 (m, 3H)
			(268.13)	found	58.22	9.11	
2b	90	1.4642	$C_{13}H_{24}O_2Si_2$	calcd	58.18	9.02	0.39 (s, 9H), 0.40 (s, 9H), 2.38 (s, 3H), 6.81−6.84 (m, 3H)
			(268.13)	found	58.25	9.07	
2c	70	1.4805	$C_{14}H_{26}O_2Si_2$	calcd	59.54	9.29	0.50 (s, 18H), 2.48 (s, 9H), 6.98 (s, 2H)
			(282.53)	found	59.55	9.28	
2d	93	1.4686	$C_{16}H_{30}O_2Si_2$	calcd	61.90	9.75	0.59 (s, 9H), 0.62 (s, 9H), 1.61 (s, 9H), 7.11−7.19 (m, 3H)
			(310.58)	found	61.79	9.68	
2e	91	1.4765	$C_{17}H_{32}O_2Si_2$	calcd	62.93	9.95	0.22 (s, 9H), 0.28 (s, 9H), 1.26 (s, 9H), 2.18 (s, 3H), 6.71−6.73 (m, 2H)
			(324.19)	found	63.02	9.98	
2f	98	70−71	$C_{20}H_{38}O_2Si_2$	calcd	65.53	10.46	0.26 (s, 9H), 0.38 (s, 9H), 1.27 (s, 9H), 1.40 (s, 9H), 6.78−6.89 (m, 2H)
			(366.69)	found	65.55	10.39	
2g	95	56−57	$C_{16}H_{24}O_2Si_2$	calcd	63.13	7.95	0:22 (s, 18H), 6.62−6.82 (m, 6H)
			(204.54)	found	63.22	7.98	
7	50	1.4828	$C_{15}H_{28}O_2Si_2$	calcd	60.78	9.53	0.24 (s, 18H), 2.08 (s, 3H), 2.11 (s, 3H), 2.13 (s, 3H), 6.45 (s, 1H)
			(296.16)	found	60.80	9.55	

4-Nitro-*N*-phenylphthalimide (**3b**) was prepared analogously. Yield: 82%. Mp: 193−194 °C (lit. mp: 192.5−194 °C[13]).

3-Morpholinomethyl-5-*tert*-butylcatechol. *tert*-Butylcatechol (0.5 mol) was dissolved in a mixture of ethanol (50 mL) and morpholine (0.5 mol). A 35 wt % aqueous solution of formaldehyde was added dropwise, and the reaction mixture was stirred for 20 h. The precipitated product was then isolated by filtration, dried, and recrystallized from 2-propanol. Yield: 91%. Mp: 153−154 °C. Anal. Calcd for $C_{15}H_{23}NO_3$ (265.35): C, 67.90; H, 8.74; N, 5.28. Found: C, 67.83; H, 8.77; N, 5.22. ^{1}H NMR (DMSO-d_6/TMS): δ 1.20 (s, 9H), 2.45 (t, 4H), 3.59 (t, 4H), 6.52−6.72 (m, 2H), 9.19 (s, 2H).

3-Acetoxymethyl-5-*tert*-butylcatechol Bisacetate. 3-Morpholinomethyl-5-*tert*-butylcatechol bis (0.1 mol) was refluxed in acetic anhydride (100 mL) for 18 h. About 20 mL of the reaction medium were evaporated in vacuo, and the remaining solution was cooled in a refrigerator. The precipitated product was isolated by filtration and recrystallized from a toluene/ligroin mixture (volume ratio 1:1). Yield: 71%. Mp: 93−94 °C. Anal. Calcd for $C_{17}H_{22}O_6$ (322.36): C, 63.34; H, 6.88. Found: C, 63.32; H, 6.88. ^{1}H NMR ($CDCl_3$/TMS): δ 1.31 (s, 9H), 2.06 (s, 3H), 2.28 (s, 3H), 2.30 (s, 3H), 5.06 (s, 2H), 7.16−7.32 (m, 2H).

3-Bromomethyl-5-*tert*-butylcatechol Bisacetate. 3-Acetoxymethyl-5-*tert*-butylcatechol bisacetate (0.1 mol) was dissolved in dry CH_2Cl_2 (180 mL), and 100 mL of a 33 wt % solution of HBr in acetic acid was added slowly with stirring. The product which had precipated after a storage of 20 h at 20 °C was filtered off, washed with a small amount of cold CH_2Cl_2, and recrystallized from hexane. Yield: 85%. Mp: 112−114 °C. Anal. Calcd for $C_{15}H_{19}BrO4$ (343.22): C, 52.49; H, 5.58; Br, 23.28. Found: C, 52.45; H, 5.56; Br, 23.13. ^{1}H NMR ($CDCl_3$/TMS): δ 1.31 (s, 9H), 2.28 (s, 3H), 2.35 (s, 3H), 4.41 (s, 2H), 7.15−7.30 (m, 2H).

3-Methyl-5-*tert*-butylcatechol (9). 3-Bromomethyl-5-*tert*-butylcatechol bisacetate (50 mmol) was dissolved in a mixture of dry THF (100 mL) and glacial acetic acid (300 mL). Zinc powder (170 mmol) was added, and this suspension was refluxed under nitrogen for 8 h. The cold solution was filtered off and evaporated. The residue was refluxed with stirring for 4 h in a mixture of methanol (200 mL) and concentrated HCl (4 mL). The cold reaction mixture was neutralized with solid $NaHCO_3$, filtered, and evaporated. The product was extracted from the residue by hot hexane. The combined hexane extracts were concentrated to a volume of approximately 200 mL and the product that had crystallized after cooling was isolated. This product was silylated (see below) without additional purification.

3,6-Dimethylcatechol (8). This product was prepared from catechol analogously to 3-methyl-5-*tert*-butylcatechol. It was immediately silylated, and the bistrimethylsilyl derivative was characterized (Table 1).

Silylation of the Catechols. A solution of triethylamine (0.22 mol) in dry toluene (60 mL) was added dropwise with stirring to a warm solution of a catechol (0.1 mol) and chlorotrimethylsilane (0.22 mol) in dry toluene (200 mL). The reaction mixture was refluxed for 4 h, cooled with ice, and filtered with exclusion of moisture. The filtrate was concentrated in vacuo, and the silylated catechol was isolated by distillation at a vacuum of 0.01 mbar (yields and properties see Table 1).

Silylation of 3,5-Bis(*tert*-butyl)catechol (2f). 3,5-Bis(*tert*-butyl)catechol (0.15 mol) was silylated as described above, but because of steric hindrance only a monotrimethylsilyl derivative was isolated. Yield: 96%, $n_D^{20} = 1.4877$. Anal. Calcd for $C_{17}H_{30}O_2Si$ (294.5): C, 69.33; H, 10.27. Found: C, 69.29; H, 10.28.

This monosilylated compound (0.1 mol) was dissolved in 300 mL of dry toluene at 80 °C, and a solution of *N*-butyllithium (0.1 mol) in dry toluene (100 mL) was added dropwise. The stirring was continued at 80 °C for 0.5 h. Afterward, chlorotrimethylsilane (0.16 mol) was added dropwise, and the reaction mixture was refluxed for 4 h. After cooling, the reaction mixture was filtered under exclusion of moisture, the filtrate was concentrated in vacuo, and the product was isolated by distillation in vacuo (for yields and properties see Table 1).

Bis(ether phthalimide)s (4a−g, 10). (**A**) **Substitution of 4-Chloro-*N*-phenylphthalimide (3a).** A silylated catechol (0.05 mol) and 4-chloro-*N*-phenylphthalimide (0.11 mol) were dissolved in dry NMP (100 mL), and dry K_2CO_3 (0.065 mol) or KF (0.13 mol) were added. This mixture was stirred at 120 °C for 24 h. After cooling, the reaction mixture was poured into cold water (1.5 L). The precipitated product was isolated by filtration, washed with water and cold methanol, and recrystallized (for yields and properties see Table 2).

(B) Substitution of 4-Nitro-*N*-phenylphthalimide (3b). When **3b** was used as reaction partner of the silylated catechols **2b** and **2d** according to procedure A (see above), bis(ether imide) **4b** was isolated in a yield of 59% and bis(ether imide) **4d**, in a yield of 62%. Their properties were identical with those of the bis(ether imide)s prepared from **3a** (see Table 2).

Bis(ether anhydride)s (6a−f, 11). A bis(ether imide) such as **4a** (20 mmol) was refluxed with stirring in a mixture of water (400 mL), methanol (80 mL), and KOH (100 g). A clear solution was obtained after 3−4 h, and the heating was continued for 45 h. Both methanol and aniline were removed by distillation under normal pressure, the remaining alkaline solution was diluted with cold water (1 L) and acidified to pH 1−2 with concentrated HCl. The precipitated tetracarboxylic acid was filtered off, washed with water and dried at 60 °C in vacuo. The crude tetracarboxylic acid (10 mmol) was suspended in a mixture of glacial acetic acid (30 mL) and acetic anhydride (30 mL). This mixture was refluxed for 1 h and allowed to cool slowly to 20 °C. The precipitated dianhydride was filtered off and recrystallized (see Table 3).

Table 2. Yields and Properties of the Bis(ether imide)s

bis(ether imide)	yield (%)	mp (°C)	solvent for recryst	mol formula (mol wt)	elemental analyses				^{1}H NMR ($CDCl_3$/TMS), δ(ppm)
						C	H	N	
4a	42	302−303	dioxane/CH_3CN (4/1; v/v)	$C_{35}H_{22}N_2O_6$ (566.57)	calcd	74.20	3.91	4.94	2.31 (s, 3H), 7.09−7.88 (m, 19H)
					found	73.87	4.06	4.96	
4b	37	233	toluene	$C_{35}H_{22}N_2O_6$ (566.57)	calcd	74.20	3.91	4.94	2.45 (s, 3H), 7.08−7.87 (m, 19H)
					found	74.11	3.92	4.98	
4c	41	268	toluene	$C_{36}H_{24}N_2O_6$ (580.60)	calcd	74.47	4.17	4.82	2.22 (s, 6H), 7.01−7.88 (m, 18H)
					found	74.05	4.91	4.28	
4d	46	156−158	toluene	$C_{38}H_{29}N_2O_6$ (609.66)	calcd	74.86	4.79	4.59	1.39 (s, 9H), 7.08−7.87 (m, 19H)
					found	74.65	4.71	4.56	
4e	44	209−210	toluene	$C_{39}H_{30}N_2O_6$ (622.68)	calcd	75.23	4.86	4.50	1.38 (s, 9H), 2.25 (s, 3H), 7.05−7.87 (m, 18H)
					found	74.57	4.98	4.53	
4f	43	167−169	methanol	$C_{42}H_{36}N_2O_6$ (664.76)	calcd	75.89	5.46	4.21	1.39 (s, 18H), 6.87−7.87 (m, 18H)
					found	75.18	5.49	4.20	
4g	57	269−270	toluene	$C_{38}H_{22}N_2O_6$ (602.60)	calcd	75.74	3.68	4.65	6.88−7.88 (m, 22H)
					found	75.08	3.71	4.48	
10	79	318−319	dioxane	$C_{37}H_{26}N_2O_6$ (594.62)	calcd	74.74	4.43	4.71	2.13 (s, 9H), 6.86 (s, 1H), 7.35−7.97 (m, 16H)
					found	73.85	4.40	4.82	

Table 3. Yields and Properties of the Bis(ether anhydride)s

dianhydride	yield (%)	mp (°C)	solvent for recryst^a	mol formula (mol wt)	elemental analyses		
						C	H
6a	98	209−210 (208−209[10b])	Ac_2O/CH_3CN (1:1)				
6b	98	191−192 (179−180[10b])	Ac_2O/CH_3CN (1:3)				
6c	98	247−248	Ac_2O/CH_3CN (1:1)	$C_{24}H_{14}O_8$ (430.37)	calcd	66.98	3.28
					found	66.52	3.27
6d	97	188−189 (158−159[10b])	Ac_2O/CH_3CN (1:9)				
6e	98	179−181	Ac_2O/CH_3CN (1:5)	$C_{27}H_{20}O_8$ (472.45)	calcd	68.64	4.27
					found	68.30	4.16
6f	81	159−160 (147−148[10b])	Ac_2O/CH_3CN (1:6)				
6g	76	262−263 (264−265[10b])	Ac_2O/AcOH (1:1)				
12	97	243−244	Ac_2O/CH_3CN (2:1)	$C_{25}H_{16}O_8$ (444.40)	calcd	67.57	3.63
					found	67.53	3.68

^{a} Ac_2O = acetic anhydride, AcOH = acetic acid.

Bis(ether anhydride) (6g). 2,3-Bis(3,4-dicarboxyphenoxy)-naphthalene (5 mmol) was refluxed in acetic anhydride (30 mL) for 1 h; the product that precipitated after cooling was filtered off and recrystallized from a mixture of glacial acetic acid/acetic anhydride (volume ratio 1:1, see Table 3).

Polycondensations. A bis(ether phthalic anhydride) (2.5 mmol) and an aromatic diamine (2.5 mmol) were weighed under nitrogen into a 25 mL round-bottom flask and stirred with dry NMP (5 mL) for 24 h at 20 °C. Afterward, dry NMP (10 mL), acetic anhydride (10 mmol) and triethylamine (10 mmol) were added, and the stirring was continued for 24 h. The reaction mixture was then poured into methanol (500 mL). The precipitated polyimide was isolated by filtration and dried in vacuo. Finally, the polyimide was dissolved in CH_2Cl_2 (and TFA if necessary) and precipitated again into methanol.

Measurements. The inherent viscosities were measured with an automated Ubbelohde viscometer at 20 °C. Differential scanning calorimetry (DSC) was conducted with a Perkin-Elmer DSC-7 at a heating rate of 20 °C/min. The infrared (IR) spectra were recorded with a Nicolet SXB-20 FT-IR spectrometer from KBr pellets. ^{1}H NMR spectra were recorded with a Bruker AC-100 FT NMR spectrometer in $CDCl_3$ using TMS as internal standard. The thermogravimetric analyses (TGA) were conducted with a Netzsch TG209 at a heating rate of 10 °C/min in an argon atmosphere. Gas permeation data were measured as follows. Solvent-free films about 15−50 μm in thickness were prepared (see ref 14). Pure gases were applied using a self-built vacuum time-lag apparatus[15] connected to a turbo molecular pump to generate an oil-free vacuum. The permeate pressure increase with time was recorded at 30 °C by two MKS Baratron pressure sensors (10 mbar maximum (permeate), 1 bar maximum (feed)) that were connected directly to a computer. Software developed in the Labview environment ensures automated measurements. Typically, the total time of measurement is set to four time-lags with an automatically adapting data sampling rate to yield 600 data points. For H_2 and He, usually only 200 data points measured at a speed of 20 data points/s are necessary to describe time-lag and steady-state gas transport completely. Time-lags below 1 s can be detected and reproduced precisely. Feed pressure was varied from 0.1 to 1 bar. Permeate pressure was $<10^{-4}$ mbar at the beginning of the experiment and was recorded up to 0.05−9 mbar, depending on the feed gas. The gases were measured in the following order: He, H_2, N_2, O_2, CO_2, and CH_4. Permeability was calculated from the slope of the permeate pressure versus time data in the steady-state region. Apparent diffusion coefficients, D_a, were estimated from the time-lag θ by $D_a = l^2/6\theta$ (l being the film thickness). Apparent solubility coefficients, S_a, were calculated from $S_a = P/D_a$. Selectivities of P and D_a, S_a, were calculated by $X(a/b) = X_a/X_b$.

Results and Discussion

Syntheses of Monomers. In previous studies it was found that syntheses of ethers from silylated phenols and alkyl bromides or alkylsulfonates give higher yields than syntheses based on the alkali salts of the phenols.[16] Furthermore, numerous high molecular weight polyethers were prepared in high yields by polycondensations of silylated diphenols with activated fluoroaromats[17] chloroaromats[18] or alkane bis(sulfonate)s.[19] On the basis of these results a new approach to the syntheses of the bis(ether anhydride)s **1** was designed

Scheme 1. Synthesis of Substituted Catechols 8, 9

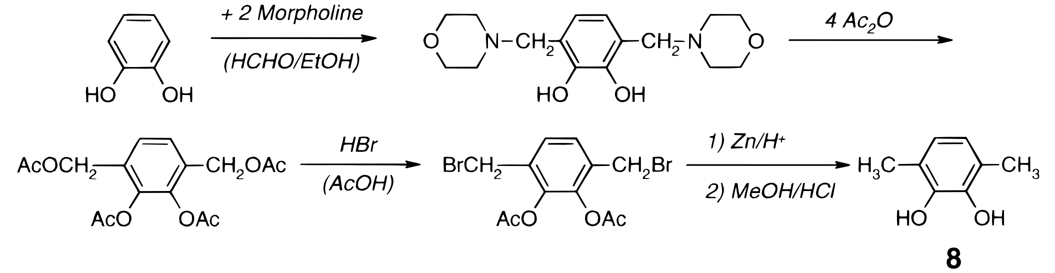

along the reaction pathway of eqs 1−3. The silylated

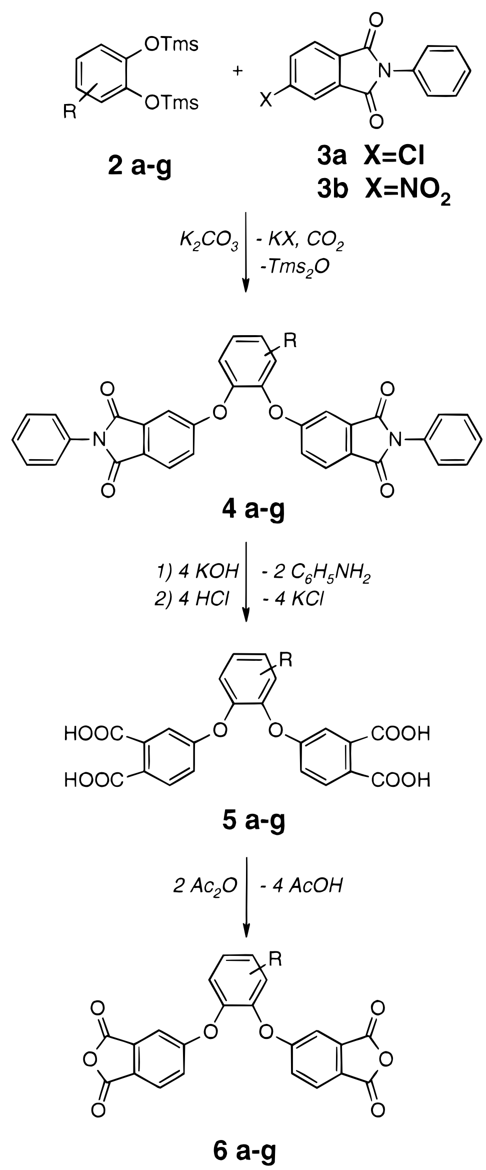

(1)

(2)

(3)

catechols **2a**−**g** in combination with K_2CO_3 or KF should be used as nucleophilic reaction partners of 4-chloro-*N*-phenylphthalimide (**3a**) or 4-nitro-*N*-phenylphthalimide (**3b**). The hydrolysis of the resulting bis(ether imide)s **4a**−**g** followed by the dehydration of the tetracarboxylic acids **5a**−**g** should yield the desired bis(ether anhydride)s **6a**−**g**.

The catechols needed for the preparation of the bistrimethylsilylderivatives **2a**−**g** and **7** were commercially available, but two compounds (**8** and **9**) had to be synthesized. The 3,6-dimethylcatechol **8** was prepared

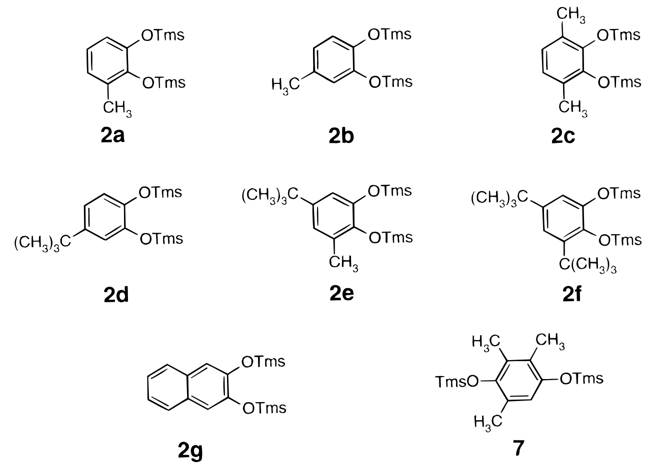

from unsubstituted catechol according to Scheme 1 following procedures in the literature.[20−22] The 3-methyl-5-*tert*-butylcatechol **9** was prepared analogously starting out from 4-*tert*-butylcatechol (eq 4).

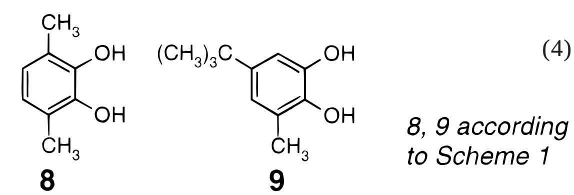

(4)

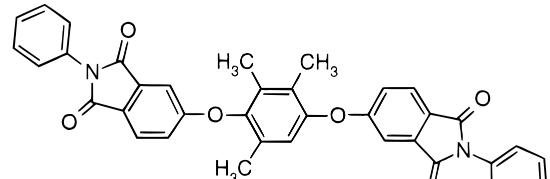

10

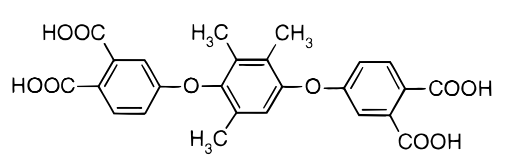

11

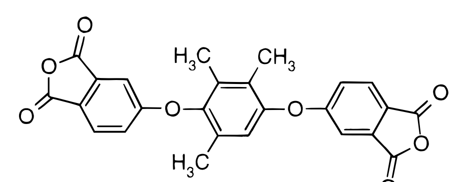

12

Scheme 2. Diamines Used in the Polyimide Syntheses

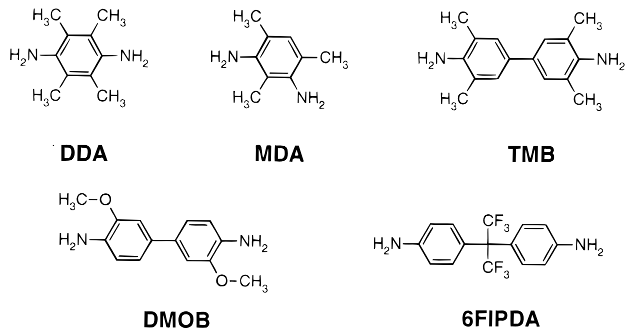

For the syntheses of the bis(ether imide)s **4b** and **4d** the following comparative studies were conducted. *First*, the usefulness of the 4-chlorophthalimide **3a** and that of the 4-nitrophthalimide **3b** were compared. Using K_2CO_3 as catalyst and base, **4b** and **4d** were obtained in yields of 37 and 46%, respectively, when **3a** served as starting material. With **3b**, however, the yields were 59 and 67%. From the fundamental studies of Williames[13,23] it is known that the reactivity of the 4-nitrophthalimide in ether syntheses should be 130 times higher than that of the 4-chlorophthalimide. The higher yields obtained with **3b** reflect this higher reactivity. However, the products derived from **3b** had a yellowish color even after recrystallization suggesting that the nitrite ion causes side reactions under the reaction conditions used in this work. For this reason and because of the lower costs of 4-chlorophthalic acid, **3a** was used for all other syntheses (see Table 2). *Second*, the syntheses of **4b** and **4d** from **3a** were conducted with KF as catalyst and base. Yields of 45 and 52%, respectively, were found, indicating that KF is advantageous over K_2CO_3 in these syntheses. Just for reasons of costs K_2CO_3 was used for all further syntheses of bis(ether imide)s. Their yields and properties are summarized in Table 2. The bis(ether imide)s **4a**−**g** and **10** were hydrolyzed with concentrated aqueous KOH (eq 2) and the crude tetracarboxylic acids **5a**−**g** and **11** were cyclized by means of hot acetic anhydride. The resulting bis(ether anhydride)s **6a**−**g** and **12** were recrystallized prior to their characterization. Their yields and properties are summarized in Table 3. In two cases the melting points were significantly higher than those reported in the literature.[10b] Furthermore, two new bis(ether anhydride)s **6c**,**f** were isolated. The bis(ether anhydride) **12** was included in this study to enable a comparison between poly(ether imide)s derived from substituted catechols and from a substituted hydroquinone with hindered rotation around the ether bonds.

Syntheses of Polyimides. All polyimides were prepared via the same procedure. The five diamines (mesitylene diamine (MDA), durene diamine (DDA), tetramethylbenzidine (TMB), dimethoxybenzidine (DMOB), and (hexafluoroisopropylidene) dianiline (6FIPDA) used as reaction partners of the bis(ether anhydride)s are summarized in Scheme 2. A diamine and a bis(ether anhydride) were reacted in dry NMP at 25 °C for 24 h (eq 5), and the cyclization of the resulting polyamic acid was achieved by addition of acetic anhydride and triethylamine (eq 6). The completeness of the imidization was checked by IR spectroscopy. The IR spectrum exemplary shown in Figure 1 demonstrates the absence of NH vibrations in the range of 3000−3500 cm^{-1} and amide I (1660 cm^{-1}) and amide II (1520 cm^{-1}) bands found in the amic acid before cyclization. The codes of the 21 isolated polyimides (**A*n*** to **H*n***), their yields, and their properties are listed in Table 4.

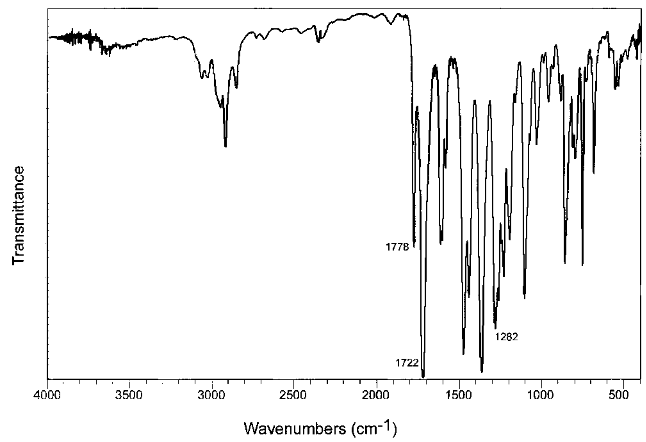

Figure 1. IR spectra from polyimide **A3**.

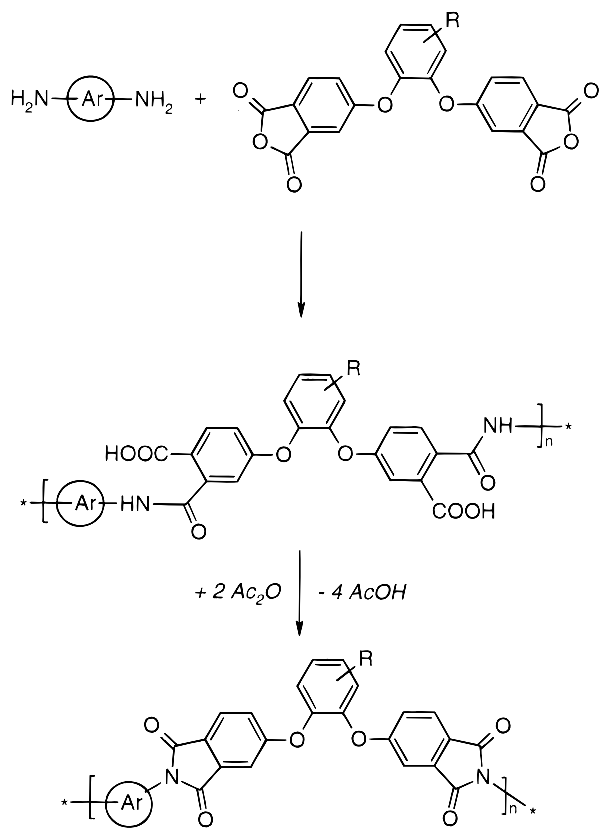

(5)

(6)

Properties of the Polyimides. Solubility. For the use of polymers as membrane materials mechanically stable films of variable thicknesses are required. Usually, casting from solvents is applied to form the membrane. Solubility in high boiling solvents to cast asymmetric membranes and in low boiling solvents to form thin film composite membranes is desirable. All the polymers were soluble in mixtures of CH_2Cl_2/TFA (4:1). Most of the polymers were additionally soluble in high (e.g., NMP) and low boiling (halogenated hydro-

Table 4. Yields and Properties of the Polyimides

polyimide	dianhydride	diamine	yield (%)	mol formula (mol wt)	elemental analyses	C	H	N	η_{inh}[a] (dL/g)	solubility NMP	$CHCl_3$	THF	mix[b]	film from solvent[c]	TGA − 10%[d]
A1	**6a**	DDA	92	$C_{33}H_{24}N_2O_6$	calcd	72.79	4.44	5.14	0.91	+	+	+	+	NMP	486
				(544.56)	found	71.18	4.44	5.13							
A2	**6a**	MDA	90	$C_{32}H_{22}N_2O_6$	calcd	72.45	4.18	5.28	0.75	+	+	+	+	−	501
				(530.54)	found	71.25	4.11	5.19							
A3	**6a**	TMB	95	$C_{39}H_{28}N_2O_6$	calcd	75.74	4.55	4.51	0.75	−	−	−	+	−	−
				(620.66)	found	74.57	4.55	4.55							
B1	**6b**	DDA	97	$C_{33}H_{24}N_2O_6$	calcd	72.79	4.44	5.14	1.18	+	+	+	+	NMP	503
				(544.56)	found	71.29	4.29	4.90							
B2	**6b**	MDA	90	$C_{32}H_{22}N_2O_6$	calcd	72.45	4.18	5.28	0.84	+	+	+	+	NMP	514
				(530.54)	found	71.54	4.13	5.28							
B3	**6b**	TMB	82	$C_{39}H_{28}N_2O_6$	calcd	75.47	4.55	4.51	0.70	−	−	−	+	−	506
				(620.66)	found	74.73	4.51	4.33							
C1	**6c**	DDA	97	$C_{34}H_{26}N_2O_6$	calcd	73.11	4.69	5.02	0.61	+	+	+	+	$CHCl_3$	487
				(558.59)	found	71.98	4.60	4.84							
D1	**6d**	DDA	89	$C_{36}H_{30}N_2O_6$	calcd	73.71	5.15	4.78	0.62	+	+	+	+	NMP	510
				(586.64)	found	72.69	5.15	4.62							
D2	**6d**	MDA	89	$C_{35}H_{28}N_2O_6$	calcd	73.41	4.93	4.89	0.67	+	+	+	+	$CHCl_3$	513
				(572.62)	found	72.51	4.85	4.80							
D3	**6d**	TMB	94	$C_{42}H_{34}N_2O_6$	calcd	76.12	5.14	4.23	0.70	−	−	−	+	−	−
				(662.74)	found	75.57	5.16	4.28							
D4	**6d**	DMOB	88	$C_{40}H_{30}N_2O_8$	calcd	72.06	4.54	4.48	0.89	+	+	+	+	NMP	489
				(666.69)	found	71.30	4.48	4.16							
E1	**6e**	DDA	95	$C_{37}H_{32}N_2O_6$	calcd	73.99	5.37	4.66	0.78	+	+	+	+	NMP	−
				(600.67)	found	72.79	5.34	4.38							
F1	**6f**	DDA	96	$C_{40}H_{37}N_2O_6$	calcd	74.86	5.81	4.37	0.52	+	+	+	+	−	−
				(641.74)	found	73.94	5.89	4.15							
F3	**6f**	TMB	94	$C_{46}H_{42}N_2O_6$	calcd	76.86	5.89	3.90	0.55	+	+	+	+	−	−
				(718.85)	found	76.01	5.89	3.65							
G1	**6g**	DDA	91	$C_{36}H_{24}N_2O_6$	calcd	74.74	4.17	4.83	0.30	+	+	+	+	−	−
				(580.60)	found	73.33	4.07	4.74							
G2	**6g**	MDA	88	$C_{35}H_{22}N_2O_6$	calcd	74.20	3.91	4.94	0.20	+	+	+	+	−	−
				(566.57)	found	73.97	3.82	4.75							
G3	**6g**	TMB	92	$C_{42}H_{28}N_2O_6$	calcd	76.82	4.30	4.27	0.46	+	+	+	+	−	−
				(656.69)	found	75.79	4.21	4.25							
H1	**12**	DDA	91	$C_{35}H_{28}N_2O_6$	calcd	73.41	4.93	4.89	0.82	−	−	−	+	*m*-cresol	497
				(572.62)	found	71.97	4.83	4.88							
H2	**12**	MDA	94	$C_{34}H_{26}N_2O_6$	calcd	73.11	4.69	5.02	0.52	+	+	+	+	NMP	491
				(558.59)	found	71.64	4.63	4.83							
H3	**12**	TMB	96	$C_{41}H_{32}N_2O_6$	calcd	75.91	4.97	4.32	0.75	−	+	−	+	$CHCl_3$	491
				(648.71)	found	75.16	4.95	4.33							
H5	**12**	6FIPDA	90	$C_{40}H_{24}F_6N_2O_6$	calcd	64.69	3.26	3.77	0.57	+	+	+	+	NMP	−
				(742.63)	found	63.92	3.25	3.54							

[a] Inherent viscosities (η_{inh}) were measured at 20 °C at a concentration of 2 g/L in CH_2Cl_2/TFA (volume ratio 4:1). [b] Mixture of CH_2Cl_2/TFA (volume ratio 4:1). [c] Films used for gas permeation measurements. [d] Thermogravimetric analyses recorded at 10 °C/min in Ar at 10% weight loss.

carbons, ketones, THF) solvents (see Table 4). Introduction of the tetramethylbenzidine unit (TMB), however, resulted in insoluble polymers (**A3**, **B3**, **D3**) from the dianhydrides **6a**,**b**,**d** although the structural similar unit 1,4-diaminotetramethylbenzene (DDA) yielded soluble polymers. The solubility of the TMB containing *o*-polyetherimides **F3**, **G3** may be explained by their lower inherent viscosity (Table 4). The *p*-polyetherimides **H1**−**3**,**5** showed solubility for the meta-connected MDA and the 6FIPDA; the DDA unit caused insolubility except in the mixed solvent and in *m*-cresol. Surprisingly, introduction of the TMB unit resulted in a polymer soluble in $CHCl_3$ but insoluble in NMP.

Film-Forming Properties and Thermal Stability. To measure polymer properties from films, it is desirable to cast all the films from the same solvent. Several attempts to use the solvent mix (CH_2Cl_2/TFA (4:1)) for film preparation resulted in turbid films even with carefully adjusted evaporation conditions. Most probably, the solvent composition changed during evaporation, a phase inversion resulted, and the polymer precipitated from solution partly before a homogeneous film was obtained. Films were therefore made from NMP or $CHCl_3$. In the case of the otherwise insoluble polymer **H1** *m*-cresol was used for film formation. The polymers from dianhydride **6f**,**g** (**F1**,**2**; **G1**−**3**) showed relatively low viscosity numbers (0.2−0.55 dL/g) and in no case were defect-free, mechanically stable films obtained. In total, defect free films of 12 polymers were obtained as listed in Table 4 and used for the gas permeation experiments. The film thicknesses spanned from 13 to 60 μm. All the films were tough and flexible and therefore suited for membranes. The TGA values, recorded at 10 °C/min in Ar at 10% weight loss were between 486 and 514 °C demonstrating the high thermal stability of these polymers. Glass-transition temperatures were not clearly detectable by DSC measurements, and thus, were not reported.

Gas Separation Properties. To the best of our knowledge, gas separation properties of ortho-linked PEI were not reported so far. To compare the effect of the ether bond linkages some substituted para-linked PEI were synthesized and included together with the few data reported for comparable PEI.[24,25] For easier tracing back the polymer code to the gas permeation data and the structures, Scheme 3 summarizes formulas and polymer codes of the polymers used for the gas permeation experiments and data from literature. The structures were ordered according to the increasing sterical hindrance for the ortho-linked PEI from: **A** (3-methyl), **B** (4-methyl), **C** (3,6-dimethyl), **D** (4-*tert*-butyl), and **E** (3-methyl-5-*tert*-butyl). The para-linked PEI are the not substituted **I**[25] the trimethyl-substituted **H**[29] or the di-*tert*-butyl-substituted **J**.[24] As diamine units of the PEIs were selected: **1** (DDA, *p*-tetramethyl), **2** (MDA, *m*-trimethyl), **3** (TMB, tetramethylbiphenyl), and **4** (DMOB, dimethoxybiphenyl) representing diamines with bulky groups, hindering sterically the rotation

Scheme 3. Structures of the Polyimides Discussed in Relation to Their Gas Permeation Properties

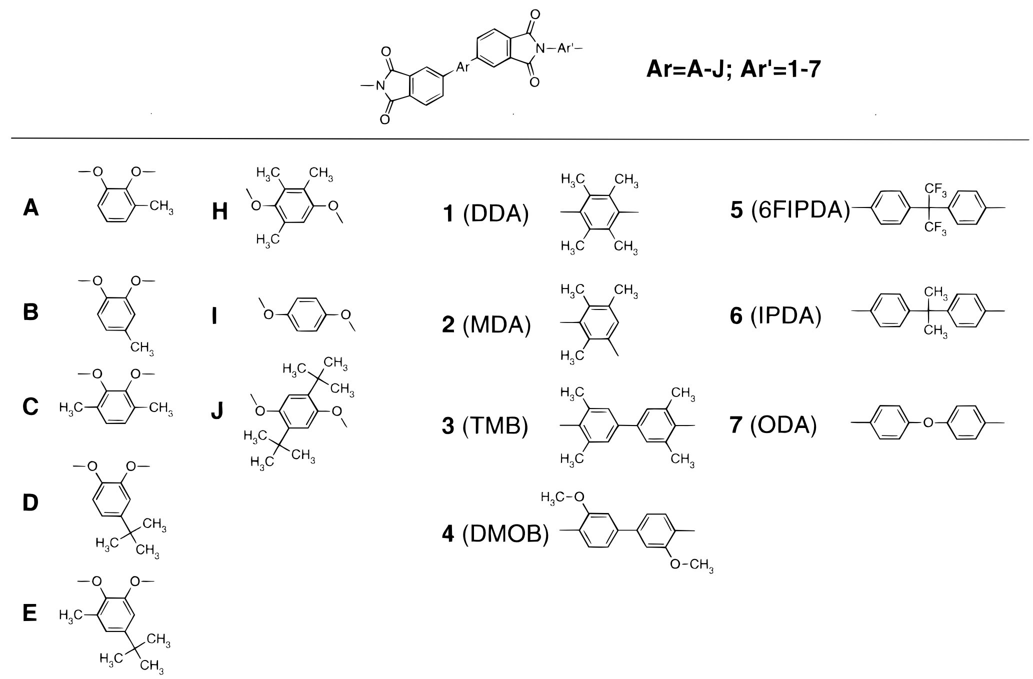

Table 5. Permeabilites[a] of the Polymers to Pure Gases

polymer code	P(He)	P(H_2)	P(CO_2)	P(O_2)	P(N_2)	P(CH_4)
A1	41	51	27	4.8	0.83	0.70
B1	33	41	20	3.5	0.59	0.47
C1	72	100	63	11	2.05	1.9
D1	64	91	71	12	2.55	3.1
E1	84	110	67	13	2.5	2.2
H1	95	230	200	33	8.1	7.6
B2	34	41	22	3.9	0.65	0.57
D2	63	85	63	11	2.2	2.5
H2	87	130	110	18	3.8	4.0
H3	39	55	39	6.5	1.2	1.2
J3		150	95	22	4.9	5.6
D4	20	22	6.7	1.4	0.21	0.16
H5	71	77	54	9.3	1.9	1.7
H6[b]		25	7.8	2.0	0.34	0.26
I7[b]		4.0		0.22	0.034	
J7[b]		43	19	4.5	0.91	0.87

[a] Permeability (P) in cm^3 (STP) cm/cm^2 s cmHg $\times 10^{-10}$ (Barrer). [b] Data for H6, J7 from the literature;[24] data for I7 from the literature.[25]

Table 6. Ideal Selectivities of the Polymers to Some Gases

polymer code	P(O_2/N_2)	P(H_2/N_2)	P(He/N_2)	P(CO_2/N_2)	P(H_2/CH_4)	P(CO_2/CH_4)	P(N_2/CH_4)
A1	5.8	61	49	33	72	39	1.18
B1	6.0	70	57	34	86	42	1.23
C1	5.4	49	35	31	53	33	1.08
D1	4.8	36	25	28	30	23	0.83
E1	5.0	42	33	27	49	31	1.17
H1	4.1	29	12	25	31	27	1.07
B2	6.0	64	53	34	73	39	1.14
D2	5.0	39	29	29	35	26	1.12
H2	4.7	36	23	30	35	31	0.94
H3	5.5	47	33	33	45	33	0.98
J3	4.4	30		19	26	17	0.88
D4	6.7	100	98	32	140	43	1.34
H5	4.8	40	37	28	46	32	1.15
H6[a]	5.9	73		23	97	31	1.34
I7[a]	6.4	120					
J7[a]	4.9	47		21	50	22	1.05

[a] Data for H6, J7 from literature;[24] data for I7 from literature.[25]

around the imide bond,[14] isopropylidenedianiline **6** (IPDA) and its 6F-analogue **5** (6FIPDA), and finally oxydianiline **7** (ODA).

Table 5 reports permeabilities of the 12 polymers to He, H_2, CO_2, O_2, N_2, and CH_4 together with some data from the literature. The permeability in general increased with increasing substitution of the aromatic ring bearing the ether groups. To start with literature data, substitution of the para-linked **I7** with 2 *tert*-butyl groups (**J7**) yielded a drastic increase of permeability, e.g., of P(H_2) from 4 to 43 Barrer. Changing the diamine part (Ar′, Scheme 3) from ODA (**1**) to TMB (**3**), the H_2 permeability increased further from 43 (**J7**) to 146 Barrer (**J3**). Substituting the di-*tert*-butyl groups by trimethyl (**J** to **H**), the permeability decreased by about a factor of 3 (**J3**, P(H_2) = 146 Barrer; **H3**, P(H_2) = 55 Barrer). However, exchange of the TMB (**3**) for DDA (**1**) resulted in the highest value for P(H_2) = 231 Barrer within this series of polymers.

Data for six polymers from the **H** series are presented in Table 5 (**H1**, **H2**, **H3**, **H5**, **H6**). The permeability for all gases increased in the order **H6** (IPDA), **H3** (TMB), **H5** (6FIPDA), **H2** (MDA) $\simeq$ **H1** (DDA) thus confirming that with the DDA (MDA) unit highest permeability was possible.[1,15] The ortho-linked PEIs **A**−**E** and the para-linked **H** were all available with DDA (**1**) or MDA (**2**) units. Again the permeabilities with DDA or MDA unit were similar. For the DDA (**1**) unit the permeability for He, H_2 increased in the order **B** (4-methyl), **A** (3-methyl), **D** (3-*tert*-butyl), **C** (3,6-dimethyl), **E** (3-methyl-5-*tert*-butyl), **H** (para, trimethyl) from: P(He) = 33 (**B1**) to 41 (**A1**), 64 (**D1**), 72 (**C1**), 84 (**E1**), and 95 (**H1**). For the gases CO_2, O_2, and N_2, the order of permeability changed. Here, **D1** permeated similar to **E1** but faster than **C1**. In the case of CH_4, **D1** permeated faster than **C1** and **E1**. Table 6 reports selectivities calculated from the pure gas permeabilities. The selectivities spanned a relatively wide range thus proving that the change in structure corresponded to a change in gas separation properties. For example, P(O_2/N_2) reaches from 4.1 (**H1**) to 6.7 (**D4**), P(H_2/CH_4) from 19 (**J3**) to 140 (**D4**), and P(CO_2/CH_4) from 17 (**J3**) to 43 (**D4**). In Figure 2 the plot of log P(O_2/N_2) (permeability selectivity) vs log P(O_2) (permeability) is shown. This plot, introduced by Robeson,[26,27] allows an assignment of the quality of a polymer to the gas separation properties at first glance. A trade off line, based on Robeson's data,[26] is included to mark

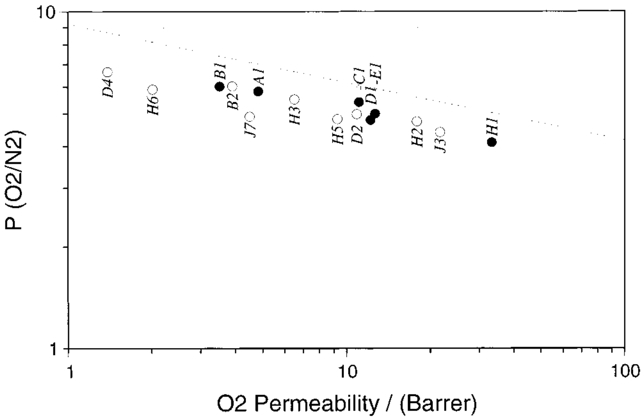

Figure 2. Relationship between O_2 permeability and O_2/N_2 permeability selectivity. Filled dots represent polymers with the DDA diamine unit **1**.

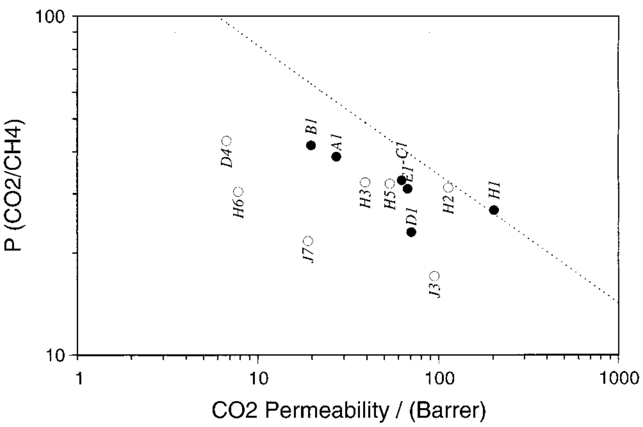

Figure 3. Relationship between CO_2 permeability and CO_2/CH_4 permeability selectivity. Filled dots represent polymers with the DDA diamine unit **1**.

the so-called "upper bound" combinations of permeability and selectivity of known polymers for oxygen/nitrogen. In this way, a measure is available with the meaning: polymers close to the line or above represent best or better membrane materials known up to now (see also discussion later and ref 28). All the polymers in Figure 2 were found below the upper bound line and are assembled mostly within a distance of about 20% below their calculated upper bound value. Exceptions are **I7** (53%), **J7** (69%), and **H2** (72%). To understand the influence of the changes of the aryl unit **A**–**E** and **H** on their gas separation quality, the polymers with the DDA (**1**) unit may be compared with respect to their approach to the upper bound. The order is as follows: **D1** (80%), **B1** (81%), **H1** (82%), **A1** (83%), **E1** (84%), and **CI** (89%). Resolved to the structure, the best performance was (in decreasing order) **C** (3,6-dimethyl), **E** (3-methyl, 5-*tert*-butyl), **A** (3-methyl), **H** (trimethyl, *p*-ether), **B** (4-methyl), and **D** (4-*tert*-butyl). As a first result, (besides that the absolute values are relatively close to each other) the *o*-ether-linked PEI with two *o*-methyl groups (**C**) is favored over the *p*-ether-linked PEI with three *o*-methyl groups (**H**). The more bulky *tert*-butyl groups alone are lower in performance for O_2/N_2 separation in the case of **D2** (47%) and **J7** (69%). In Figure 3 is shown a similar graph for the CO_2/CH_4 permeability/selectivity (for clarity the data points for **B2** and **D2** are omitted). Four polymers were identified with a performance from about 80 to 100% in correlation to the upper bound (**E1** = 78%, **C1** = 80%, **H2** = 96%, **H1** = 103%) thus proving that for CO_2/CH_4 separation PEIs with ortho-substituted *p*-ether linkages (**H**) are more effective than PEIs with ortho-substituted *o*-ether linkages (**C**). The performance of the methyl-substituted PEIs interestingly increases with increasing CO_2 permeability in the order **B**, **A**, **C**, **E**, and **H** from $P(CO_2)$ = Barrer (% relative to upper bound): **B1** = 20 (66%), **A1** = 27 (69%), **C1** = 63 (80%), **E1** = 67 (78%), **H1** = 200 (103%) (see the trend line in Figure 3). Introduction of *tert*-butyl groups (**D**, **J**) resulted in low performance for this separation problem (**D1/D2** about 60%, **J3** about 50%). Change of the Ar′ unit for *p*-PEI **H** interestingly increased the CO_2 permeability with the only minor change being in selectivity, thus increasing the performance for this separation problem with increasing permeability $P(CO_2)$ = Barrer (% relative to upper bound): **H6** = 7.8 (34%), **H2** = 39 (66%), **H5** = 54 (74%), **H2** = 110 (96%), **H1** = 200 (103%).

Table 7. Apparent Diffusivities[a] of the Polymers to Pure Gases

polymer code	D_a(He)	$D_a(H_2)$	$D_a(CO_2)$	$D_a(O_2)$	$D_a(N_2)$	$D_a(CH_4)$
A1	530	190	0.58	3.4	0.74	0.13
B1	400	180	0.47	2.9	0.62	0.11
C1	830	330	1.28	6.7	1.58	0.31
D1	690	310	1.55	7.9	2.08	0.47
E1	1100	370	1.76	7.9	1.96	0.38
H1	1300	590	3.70	14.8	4.05	0.96
B2	350	165	0.51	3.1	0.69	0.12
D2	940	330	1.52	8.0	2.10	0.50
H2	790	375	2.10	9.4	2.37	0.51
H3	330	180	0.96	3.8	0.89	0.18
D4	260	100	0.32	1.5	0.30	0.050
H5	730	260	1.42	5.5	1.34	0.31

[a] Apparent diffusion coefficient (D_a) in $cm^2/s \times 10^{-8}$.

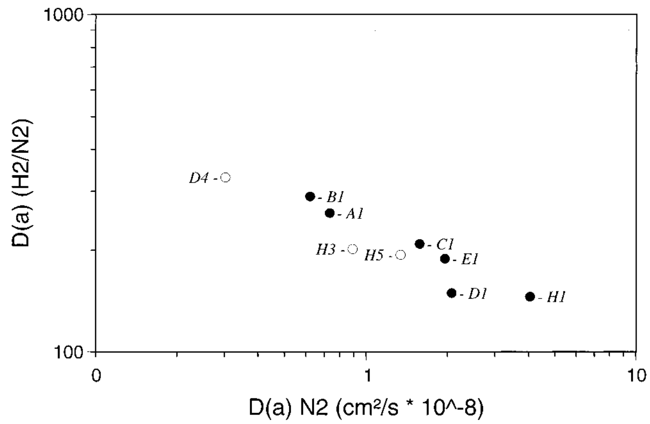

Figure 4. Relationship between N_2 apparent diffusivity and H_2/N_2 diffusivity selectivity. Filled dots represent polymers with the DDA diamine unit **1**.

Table 7 summarizes apparent diffusion coefficient (D_a) of the polymers to pure gases calculated from the time-lag. In Figure 4 apparent diffusion coefficients ($D(a)$) of N_2 was plotted with diffusion selectivity $D(a)$ (H_2/N_2). The data for **B2**, **D2**, **H2** with the diamine **2** (MDA) are very similar to the DDA diamine **1** and are omitted for clarity. As expected, the highest diffusion coefficient correlates with the lowest diffusion selectivity due to the increase in free volume. In the series **A1**–**E1** (ortho) to **H1** (para) the diffusion selectivity is similar for **H1** (para, trimethyl), **D1** (ortho, 4-*tert*-butyl)—(about 150), for **CI** (ortho, dimethyl), **E1** (ortho, 3-methyl-5-*tert*-butyl)—(about 200)—and for **A1** (ortho, 3-methyl), **B1** (ortho, 4-methyl)—(about 280). The diffusion selectivity of **H3** and **H5** is similar to **CI**, **EI** (about 200) but at a different level of diffusivity (D_a N_2: **H3** = 0.89, **H5** =

Table 8. Apparent Solubilities[a] of the Polymers to Pure Gases

polymer code	S_a(He	$S_a(H_2)$	$S_a(CO_2)$	$S_a(O_2)$	$S_a(N_2)$	$S_a(CH_4)$
A1	0.77	2.7	472	14	11	56
B1	0.83	2.3	417	12	9.4	44
C1	0.87	3.1	489	17	13	61
D1	0.93	2.9	456	15	12	65
E1	0.76	2.9	383	16	13	58
H1	0.73	3.9	549	23	20	79
B2	0.98	2.5	431	13	9.5	47
D2	0.67	2.5	410	14	11	49
H2	1.10	3.6	538	19	16	79
H3	1.19	3.1	412	17	13	68
D4	0.78	2.2	213	9.5	6.9	31
H5	0.98	3.0	379	17	14	53

[a] Apparent solubility coefficient (S_a) in cm^3 (STP)/cm^3 cmHg $\times$ 10^{-3}.

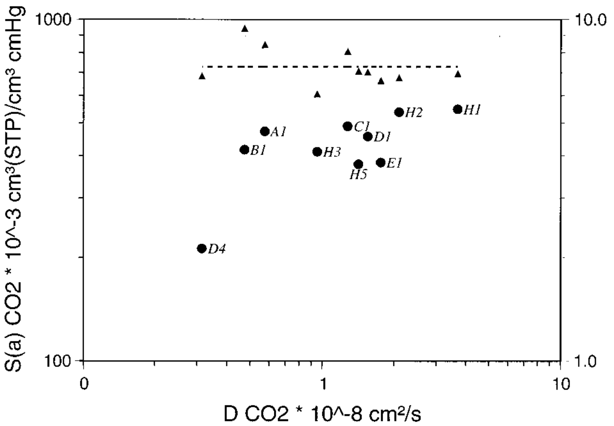

Figure 5. Relationship between CO_2 apparent diffusivity and CO_2 apparent solubility and CO_2/CH_4 solubility selectivity. The triangles represent the solubility selectivity and the dots the CO_2 solubility.

1.3, **C1** = 1.6, **E1** = 2.0 cm^2/s $\times$ 10^{-8}). Table 8 reports the calculated apparent solubilities (S_a) in order of the polymer code. In general, higher diffusivity corresponds to higher solubility. This is shown in Figure 5 where $D_a(CO_2)$ is plotted with $S_a(CO_2)$ and $S_a(CO_2/CH_4)$ on the second *y*-axis. Data points for **B2** and **D2** are close to their analogues (**B1**, **D1**) and are not drawn for clarity. A trend line inserted may indicate that there is no major change in solubility selectivity with increasing diffusion coefficient for the higher diffusing polymers (**H1**, **H2**, **E1**, **D1**(**D2**), **H5**, **C1**, **H3**; in order of decreasing $D_a(CO_2)$ and therefore $P(CO_2)$). Freeman[28] discussed the upper bound performance characteristics (developed from Robeson[26,27]) and concluded that the most fruitful pathway for development of higher performance polymers is either through solubility selectivity enhancement or an increase in chain (backbone) stiffness. Increase in backbone stiffness should be accompanied by increasing interchain separation. As a result, higher permeability may result at a higher selectivity (relative to the upper bound). In relation to the polymers tested in this series of substituted *o*- and *p*-PEIs one may conclude from Figure 3 ($P(CO_2)$ with $P(CO_2/CH_4)$) and Figure 5 ($D_a(CO_2)$ with $S_a(CO_2/CH_4)$) that increasing backbone stiffness, while maintaining or increasing interchain separation, occurs in the order

$$\mathbf{D4} < \mathbf{B1} \simeq \mathbf{A1} < \mathbf{H3} \simeq \mathbf{C1} \simeq \mathbf{H5} \simeq \mathbf{D1} \simeq \mathbf{E1} < \mathbf{H2} \simeq \mathbf{H1}$$

The best substituted *o*-PEIs (**C**, **D**, **E**) were not superior over the substituted *p*-PEI (**H**).

Conclusion

The results of the present study demonstrate, that the condensation of silylated hydrochinon or catechols with 4-chloro- or 4-nitrophthalimides is a satisfactory and relatively inexpensive approach to the synthesis of substituted "bis(ether anhydrides)". The polyimides prepared from these dianhydrides and substituted aromatic diamines are rather stiff and contain a high fraction of free volume yielding membranes with high permeabilities. Their gas separation properties are relatively close to the upper bounds defined by Robeson.[26,27] In the case of PEIs with comparable substitution patterns at the ether bonds and similar diamines, the ortho-linked PEIs are not superior in gas separation properties to their para-linked analogues.

References and Notes

(1) Langsam, M. In *Polyimides, Fundamentals and Applications*; Gosh, M. K., Mittal, K. L., Eds.; Marcel Dekker: New York, 1996; Chapter 22, p 697.
(2) Ohya, H.; Kudryavtsev, V. V.; Semenova, S. I. *Polyimide Membranes*; Gordon and Breach Publishers: Tokyo, 1996.
(3) Stern, S. A.; Mi, Y.; Yamamoto, H. *J. Polym. Sci., Part B* **1989**, *27*, 1887.
(4) Kim, T. H.; Koros, W. J.; Husk, G. R.; O'Brien, K. C. *J. Membr. Sci.* **1988**, *37*, 45.
(5) Stern, S. A. *J. Membr. Sci.* **1994**, *94*, 1.
(6) Coleman, M. R.; Koros, W. J. *J. Membr. Sci.* **1990**, *50*, 285.
(7) Hellums, M. W.; Koros, W. J.; Husk, G. R.; Paul, R. D. *J. Membr. Sci.* **1989**, *46*, 93.
(8) Muruganandam, N.; Paul, D. R. *J. Membr. Sci.* **1987**, *34*, 185.
(9) Koros, W. J.; Fleming, G. K.; Jordan, S. M.; Kim, T. H.; Hoehn, H. H. *Prog. Polym. Sci.* **1988**, *13*, 339.
(10) (a) Eastmond, G. C.; Paprotny, J. *Polymer* **1994**, *35*, 5148. (b) Eastmond, G. C.; Paprotny, J. *Macromolecules* **1995**, *28*, 2140. (c) Eastmond, G. C.; Paprotny, J. *Macromolecules* **1996**, *29*, 1382. (d) Eastmond, G. C.; Paprotny, J. *React. Funct. Polym.* **1996**, *30*, 27. (e) Eastmond, G. C.; Paprotny, J. U.S. Patent 5,434,240, 1995.
(11) McClelland, R. A.; Seaman, N. E.; Duff; J. M.; Branston, R. E. *Can. J. Chem.* **1985**, *63*, 121.
(12) Campbell, W.; Ginsig, R.; Schmid, H. *Helv. Chim. Acta* **1953**, *36*, 1489.
(13) Williams, F. J.; Donahua, P. E. *J. Org. Chem.* **1977**, *42*, 3414.
(14) Fritsch, D.; Peinemann, K.-V. *J. Membr. Sci.* **1995**, *99*, 29.
(15) Al-Masri, M.; Kricheldorf, H. R.; Fritsch, D. *Macromolecules* **1999**, *32*, 7853.
(16) Kricheldorf, H. R.; Wulff, D. *J. Polym. Sci.: Part A, Polym. Chem.* **1996**, *34*, 3511.
(17) Kricheldorf, H. R.; Bier, G. *J. Polym. Sci., Polym. Chem. Ed.* **1983**, *21*, 2283.
(18) Kricheldorf, H. R.; Jahnke, P. *Makromol. Chem.* **1990**, *191*, 2027.
(19) Kricheldorf, H. R.; Al-Masri, M. *J. Polym. Sci.: Part A, Polym. Chem.* **1996**, *34*, 2037.
(20) Caldwell, W. T.; Thompson, T. R. *J. Am. Chem. Soc.* **1939**, *61*, 2354.
(21) Sinhababu, A. K.; Borchardt, R. T. *Synth. Commun.* **1982**, *12*, 983.
(22) Fields, D. L.; Miller, J. B.; Reynolds, D. D. *J. Org. Chem.* **1964**, *29*, 2640.
(23) Williams, F. J.; Relles, H. M.; Manello, J. S.; Donahua, P. E. *J. Org. Chem.* **1977**, *42*, 3419.
(24) Eastmond, G. C.; Paprotny, J.; Richards, R. E.; Shaunak, R. *Polymer* **1994**, *35*, 4215.
(25) Ding, M.; Li, H.; Yang, Z.; Li, Y.; Zhang, J.; Wang, X. *J. Appl. Polym. Sci.* **1996**, *59*, 923.
(26) Robeson, L. M. *J. Membr. Sci.* **1991**, *62*, 165–185.
(27) Robeson, L. M.; Burgoyne, W. F.; Langsam, M.; Savoca, A.; Tien, C. F. *Polymer* **1994**, *35*, 4970.
(28) Freeman, B. D. *Macromolecules* **1999**, *32*, 375.
(29) This work.

MA9920745